N6-methyladenosine-mediated changes in SOCS3 expression regulate skeletal muscle stem cell senescence

Menghai Zhu (Zhumh@mau.edu.mk)
The Third Affiliated Hospital of Southern Medical University https://orcid.org/0000-0002-1951-0815
Chong Lian
Sun Yat-sen University First Affiliated Hospital
Gang Chen
Sun Yat-sen University First Affiliated Hospital
Peng Zou
Sun Yat-sen University First Affiliated Hospital
Beng gang Qin
Sun Yat-sen University First Affiliated Hospital

Research Article

Keywords: JAK2-STAT3 signaling, METTL3, N6-methyladenosine, skeletal muscle stem cells, suppressor of cytokine signaling 3

Posted Date: November 3rd, 2022

DOI: https://doi.org/10.21203/rs.3.rs-2087831/v1

Abstract

N6-methyladenosine (m6A)-associated mechanisms are involved in cellular metabolic activities; however, their role in skeletal muscle stem cell (SkMSC) senescence is unknown. In this study, m6A RNA modification and METTL3 expression were decreased in aged SkMSCs from mice. Transcriptional analysis of m6A modification further revealed that suppressor of cytokine signaling 3 (SOCS3) was downregulated in aged SkMSCs, and that downregulation of METTL3 promoted SkMSC senescence. In addition, the upregulation of METTL3 alleviated the senescence of SkMSCs. Mechanistically, deletion of m6A modifications promoted senescence and inhibited SOCS3 expression, whereas downregulation of SOCS3 promoted senescence. Moreover, insulin-like growth factor-2 mRNA-binding protein 1 (IGF2BP1) was identified as an important regulator in the recognition and stabilization of m6A modified SOCS3 expression. IGF2BP1 binds to SOCS3 and reinforces its stability by suppressing the phosphorylation of JAK2/STAT3. Therefore, METTL3 inhibits SkMSC senescence through m6A modification-dependent stabilization of SOCS3 expression and inhibition of JAK2-STAT3 signaling. This study thus highlights a novel mechanism underlying SkMSC senescence.

1 Introduction

The N6-methyladenosine (m6A) modification regulates transcriptional, post-transcriptional, and translational processes; thereby influencing metabolic activities such as cell proliferation, differentiation, senescence, survival, death, and various other functions[1,2]. m6A-mediated regulation has also been reported to exert its effects on advanced-aged-related diseases such as amyotrophic lateral sclerosis[3], Duchenne muscular dystrophy(DMD)[4], and sarcopenia[5,6]. Mechanistically, m6A RNA modification is regulated by a multi-component ‘writer’ complex composed of METTL3 and METTL14, which play a role in numerous physiological processes such as cell proliferation[7], differentiation[8], and senescence[9,10]. In addition, METTL3 influences the biological characteristics of various cancers by altering the m6A levels of target RNAs[11,12].

Degenerative muscle diseases, largely related to skeletal muscle stem cells (SkMSCs) and their declining proliferative ability with aging, are common age-related disorders[13,14]. Sarcopenia and Duchenne muscular dystrophy (DMD) are two of the best characterized of progerias, which are associated with significant functional impairment, such as movement retardation and muscle weakness[4,6]. Understanding the molecular mechanisms underlying advanced-age diseases is essential for developing clinical treatments for degenerative muscle diseases. Dysfunctions in RNA splicing, translation and degradation and chromatin organization contribute to cell aging. In addition, growing evidence implies that m6A modification is widely reported in senescence and post-transcriptional control is a potential therapeutic efficiency for aging rejuvenation[15–17]. Therefore, elucidating whether m6A mRNA methylation directly regulate senescence is of great significance. However, the functional role of m6A modification in SkMSC senescence remains unclear.

In this study, we employed SkMSCs from young and aged mice, to identify the potential role of m6A mRNA modifications involved in regulating SkMSC senescence. We determined the METTL3 expression levels in SkMSCs of young and aged mice, to elucidate their association with senescence. METTL3 expression was examined by q-PCR and western blotting. In addition, genetic knockdown was used to elucidate the role of METTL3 in regulating SkMSC senescence. Methylated RNA-binding protein sequencing and RNA sequencing were performed to identify the potential mechanisms underlying aging in SkMSCs. Moreover, we detected that IGF2BP1recognized and stabilized m6A-modified SOC3 to alleviated senescence. Collectively, our results provide important clues that targeting m6A modifications is a potential treatment and prevention of aging-related muscle disorders.

Our data revealed that reduction of m6A modifications was related to decreased METTL3 expression, and that aged SkMSCs with downregulated METTL3 exhibited characteristics of hastening ageing. By contrast, METTL3 upregulation promoted m6A modifications and reversed senescence in SkMSCs. To further identify specific targets of m6A modifications in aged SkMSCs, we performed RNA sequencing (RNA-seq) and m6A methylated RNA immunoprecipitation sequencing (MeRIP-seq), and discovered SOCS3 as a crucial m6A regulator, which can affect senescence.

2 Results

2.1 m6A mRNA modifications are decreased in aged SkMSCs

To elucidate the functional role of m6A in aging, we purified SkMSCs from young and aged mice, as reported previously. Aged SkMSCs showed lower proliferation (Fig. 1A, 1B) and a higher percentage of SA-β-Gal staining positive cells (Fig. 1C). A remarkable reduction in m6A levels was seen in aged SkMSCs compared with that of younger SkMSCs (Fig. 1D), as validate by immunofluorescence and LC–MS/MS (Fig. 1E, F). Similarly, METTL3 levels were decreased in aged SkMSCs (Fig. 1G). However, no significant differences were found on the expression of METTL14 between young and aged SkMSCs (Fig. 1G). Our study suggest that reduced METTL3 may contribute to the observed m6A loss in aged SkMSCs.

2.2 Reduction of METTL3 accelerated SkMSC senescence

To identify the functional role of METTL3, we knocked out METTL3 in SkMSCs (Fig. 2A). Knockout of METTL3 (METTL3-KO) reduced m6A levels (Fig. 2B). Furthermore, METTL3-KO SkMSCs developed aging phenotypes, inhibited proliferation, but enhanced percentage of SA-β-Gal-positive cells in SkMSCs (Fig. 2C, D). Therefore, METTL3-KO accelerated SkMSC senescence. Moreover, METTL3 downregulation decreased m6A levels (Fig. 2E). Subsequently, the proliferative capacity of the SkMSCs was reduced. Our results showed that decreased METTL3 accelerated SkMSC senescence and suppress cells proliferation.

2.3 Transcriptome-wide profiling of m6A modifications in young and aged SkMSCs

RNA-seq and MeRIP-seq were used to evaluate transcriptome-wide m6A in young and aged SkMSCs (Fig. 3A, B). Pearson's correlation coefficients was used to assess reproducibility, showing reliability of the MeRIP-seq data (Fig. 3A-C). Among the protein-coding mRNAs, m6A modifications were predominant (Fig. 3D), located in a consensus "DUAH" motif (D = U/G and H = C/A/U) (Fig. 3F). In addition, m6A modifications were highly enriched in the 3' untranslated regions (UTRs) and in the regions flanking stop codons (Fig. 3G, 3E).

From RNA-seq and MeRIP-seq analysis, we found that levels of genes with m6A modifications were significant highly than those without m6A modifications and were positively related to m6A levels (Figure S1A, B), implying a potential biological role of m6A in regulating of SkMSCs. In addition, decreased m6A may lead to senescence, whereas upregulated mRNAs were associated with high m6A levels (Figure S1C). This correlation located in different regions of the transcripts (Figure S1D). Therefore, our results demonstrated a positively association between m6A expression level and senescence.

2.4 Decreased m6A levels in senescence-related genes in SkMSCs.

To explore the correlation between m6A modification and SkMSC senescence, we next identified the shared and cell type-specific m6A peaks in young and aged SkMSCs (Fig. 4A, B). Shared m6A peaks (such as *Nox4*) were largely enriched in glutathione metabolism and in protein modification pathways, which are crucial for regulating cell senescence. In comparison, m6A peaks specific for aged SkMSCs were enriched in response to cytokines, protein stability, and proteasomal degradation in SkMSCs (such as *Hoxa9* and *Egr1*) (Fig. 4A, B) and in translation-related processes and RNA metabolism in SkMSCs (such as *IGF1*) (Fig. 4A, B). m6A levels were decreased in aged SkMSCs (Fig. 4A). In addition, the senescence-associated hypomethylated transcripts with m6A peaks in young SkMSCs were involved in glutathione metabolism and protein modification, most of which are related to cell senescence-related signaling(Fig. 4B). Furthermore, we found distinct patterns in the gene expression profiles of young and aged SkMSCs (Fig. 4E and Figure S1, B). In aged SkMSCs, upregulated genes were correlation with negative regulation of hydrolase activity, protein stability, proteasomal degradation, and basement membrane (Fig. 4B). In young SkMSCs, highly expressed genes were associated with regulation of exocytosis, cell cycle regulation, oxidative stress, and cell signaling and regulation (Fig. 4B, C). In addition, highly expressed genes in both young and aged SkMSCs were enriched in regulation of necrotic cell death (Figure S2A). However, genes upregulated in young SkMSCs (also meaning reduced expression genes in aged SkMSCs) were abundant in biosynthesis of unsaturated fatty acids, epithelial tube morphogenesis, histone methyltransferases, and regulation of chromosome organization (Fig. 4B, S2A), and most of these terms were related to cell senescence (Fig. 4A). Therefore, senescence-associated genes exhibiting m6A loss and downregulation were involved in SkMSC senescence (Figure S2B).

We further analyzed the m6A profiles and patterns of the METTL3-KO and control groups (Figure S3A–E) in SkMSCs. Shared m6A-modified transcripts between the METTL3-KO and METTL3-NC groups were largely abundant in processed transcripts and regulation of cell morphogenesis (Figure S3F). The m6A levels increased following down-regulation of METTL3(Figure S3E), largely attribute to the presence of m6A modification. Interestingly, regulation of protein kinase activity was also mainly due to decreased m6A modification after knock-out of METTL3 (Figure S3F), further demonstrating that decreased m6A levels and cell senescence-related genes potentially contribute to SkMSC senescence.

2.5 SOCS3 functions as a key m6A target in regulating the senescence of SkMSCs

We next aimed to identify the regulators regulating m6A-associated SkMSC senescence. A significant reduction of mRNA methylation in regions flanking the stop codons of transcripts was observed in both aged SkMSCs and SkMSCs with METTL3-KO group (Fig. 5A, B, and Figure S4A–D). Furthermore, GO analysis showed that the transcripts were enriched in senescence-related terms (Fig. 5C) and SOCS3 levels were dramatically decreased in both aged and METTL3-KO SkMSCs (Fig. 5D, S4D), as supported by MeRIP-qPCR analysis (Fig. 5E, F).

We also observed a significantly diminish in SOCS3 expression both at the mRNA and protein levels in aged SkMSCs as well as in METTL3-KO SkMSCs (Fig. 6A–D). When we examined the stability of Socs3 mRNA, we noticed a shortened mRNA half-life of SOCS3 in aged SkMSCs as well as in METTL3-KO SkMSCs (Figure S5A, B), demonstrating that decreased m6A modifications could suppressed SOCS3 mRNA stability. IGF2BP1 recognized m6A modifications and enhanced their stability, as identified through high-throughput sequencing analyses. Consequently, we investigated the functional role of IGF2BP1recognition and m6A-modified SOCSs3 mRNA stabilization in regulating SkMSC senescence.

To identify the potential interaction between IGF2BP1and SOCS3 mRNA in SkMSCs. We performed RIP-qPCR analysis with an anti-IGF2BP1 antibody and observed a marked increase in the interaction between IGF2BP1and SOCS3 mRNA (Fig. 6E). Whereas, METTL3-KO disrupted this interaction (Fig. 6F), indicating that IGF2BP1 binds to SOCS3 mRNA in a METTL3/m6A-dependent manner.

To test whether IGF2BP1 enhances SOCS3 expression, we next knocked down IGF2BP1 and found a marked reduction in SOCS3 expression at both the mRNA and protein levels (Fig. 6G–I). Moreover, we found the shortening of the SOCS3 mRNA half-life following IGF2BP1 knockdown (Figure S5C), indicating that IGF2BP1 may recognize and stabilize m6A-tagged SOCS3 mRNA.

Downregulation of SOCS3 expression in SkMSCs (Fig. 6J) reduced SOCS3-promoted SkMSC senescence, as supported by impaired proliferation and increased percentage of positive cells by SA-β-Gal staining (Fig. 6K, L). IGF2BP1 downregulated promoted cellular senescence of SkMSCs (Fig. 6M, N). Therefore, IGF2BP1 and its target SOCS3 contribute to m6A-associated regulation and promote senescence of SkMSCs.

2.6 SOCS3 suppresses SkMSCs senescence via JAK2-STAT3 signaling

To identify the molecular mechanism underlying the SOCS3-mediated inhibition of the accelerated senescence of SkMSCs, gene set enrichment analysis (GSEA) suggest the association between SOCS3 and the JAK2–STAT3 signaling pathway (Fig. 7A). Mouse phospho-kinase microarray assays were conducted to verify the signaling effects of SOCS3. SOCS3 knockdown promoted JAK2–STAT3 phosphorylation (Fig. 7B-D), whereas its upregulation reduced JAK2 phosphorylation. Western blotting revealed changes in phosphorylated JAK2 level when SOCS3 was upregulated and downregulated (Fig. 7E). Immunofluorescence confirmed these trends; JAK2 phosphorylation decreased in SOCS3-overexpressing cells (Fig. 7F). Therefore, SOCS3-mediated fluctuation in level of JAK2 phosphorylation may be the mechanism underlying senescence role of SOCS3 in SkMSCs.

Oncostatin M (OSM) can induce the activation of STAT3; this activation is inhibited by WHI-P154, a specific inhibitor of JAK2 in a dose-dependent manner. SOCS3 downregulation promoted JAK2 and STAT3 phosphorylation, whereas SOCS3 upregulation inhibited JAK2 and STAT3 phosphorylation. Therefore, SOCS3 downregulation can activate the JAK2/STAT3 signaling, whereas SOCS3 upregulation had the opposite effect. METTL3-KO SkMSCs were treated with 20 and 50 μM WHI-P154. which suppressed JAK2 and STAT3 phosphorylation. The inhibitory effects of WHI-P154 treatment were enhanced with an increase of WHI-P154 concentration in SkMSCs (Fig. 7G, H). The JAK2 phosphorylation level decreased when SkMSCs were treated with WHI-P154, and simultaneously the expression of STAT3 in the SOCS3-OE + OSM + WHI-P154 (50 μM) group was lower than that in the SOCS3-OE + OSM + WHI-P154 (20 μM) group (Fig. 7G). Inhibition of the JAK2/STAT3 signaling pathway suppressed cells proliferation and increased percentage of positive cells of SA-β-Gal staining. Therefore, SOCS3 reduces SkMSC senescence via the JAK2/STAT3 signaling pathway.

3 Discussion

Increasing evidences demonstrated that m6A mRNA modification are involved in numerous biological functions in senescence.In this study, we found that m^6A RNA modifications is heavily involved in senescence of SkMSCs. Initially, both reduction of m^6A modification and METTL3 expression were observed in aged SkMSCs. Then, we found that downregulation of METTL3 lead to m^6A modifications downregulation and SOCS3 upregulation, accelerating SkMSC senescence. Subsequently, upregulation of METTL3 enhanced m^6A modifications and inhibited senescence by the JAK2-STAT3 signaling pathway through upregulation of SOCS3 in SkMSCs. Finally, IGF2BP1 recognized and stabilized m6A-modified SOCS3 mRNA to relieve senescence of SkMSC. Collectively, our results suggest that upregulation of METTL3 and m6A modifications can relieve senescence of SkMSCs via IGF2BP1 modulating enhancement of SOCS3 mRNA stability, which disturbed the JAK2-STAT3 signaling pathway. These results not only identify the roles of m6A and

METTL3 in senescence of SkMSC, and also implied the possibility to develop therapeutic strategies for aging-related muscle disorders.

By targeting different mRNAs in young and aged SkMSCs, m6A regulation by METTL3 is involved in regulating biological processes in very different way. Aberrant expression of m^6A are known to support critical germinal center (GC) functions, cell malignant transformation and carcinogenesis through regulating the expression of targeted mRNAs[18–20]. Remarkably, abnormal m6A modifications are reported to regulate senescence, which may be implicated in age-related disorders. Moreover, dysregulation of m6A was also reported to be involved in age-related neural activity and Alzheimer's disease [21,22]. These findings imply a regulatory function of m6A in aging. Consistent with our findings, recent studies reported that METTL3 regulates m6A levels in myoblasts and in the transition of myoblasts to different cell states[12]. Decreased m^6A modifications has been reported to regulate the fate of bone marrow mesenchymal stem cells and the bone-fat balance during skeletal aging. However, the earliest stages of terminal differentiation commitment were not investigated and the upstream signal that leads to the decline in METTL3 transcription has not yet in full shape. Our study further employed young and aged SkMSCs and found m^6A loss in aged SkMSCs due to reduction of METTL3. Moreover, knockout of METTL3 was observed to accelerate senescence in SkMSCs, implying METTL3 as well as m^6A play important roles in the senescence of SkMSCs. Similar to our study, Li also reported that METTL3 deficiency shortens the lifespan in Drosophila[23].

In aged SkMSCs, m6A profiling observed the declined methylation and protein coding pathways. Protein coding is a general stereotypes in aging. As a protein coding regulator, SOCS3 can directly interact with JAK2, suppressing the JAK2/STAT3 signaling pathway and thus plays roles in regulating cell signaling connectivity under physiological and pathological conditions.[24–26]. Consistently, reduction of SOCS3expression in cells causes abnormal epigenetic and metabolic reprogramming[27,28]. Recent studies reported that decreased m6A methylation results in a reduction of SOCS3 mRNA[29–31]. However, regulatory mechanism of SOCS3 in senescence still remains uninvestigated. Our study identified the reduction of m^6A modification and SOCS3 and its association in aged mouse SkMSCs. METTL3 knockout decreased the stability of SOCS3, may owe to reduced m6A modifications around their stop codons preferentially recognized and stabilized by IGF2BP1[32–34]. Really, numerous studies suggest that IGF2BP1 selectively recognizes and promotes mRNA stability[35,36]. Our data demonstrated that m6A modification and SOCS3 are involved senescence of SkMSCs, suggesting that intervention of m6A modification and m6A might be a potential strategy for regulating cell senescence.

SOCS3 function as a negative regulator of the JAK-STAT pathway, which plays a crucial role in age-related diseases and cellular aging[37,38]. The role of SOCS3 in aging regulation is achieved by inhibiting JAK-STAT pathway, and other related mediators. SOCS3can bind to JAK2 and suppress the activation of STAT3, thereby regulating cellular aging. Recent studies have reported that SOCS3 has a detrimental role of inflammation and that reduction of SOCS3 can cause primary microglial dysfunction and the development age-related retinal microgliopathy in mice[38]. In addition, knock out of SOCS3 in mice can

restrain cell proliferation and growth. In a mouse model, METTL3 was reported to modify SOCS3 mRNAs by m6A methylation, which decreased the degradation of SOCS3 and increased its translation, thereby suppressing JAK2/STAT3 signaling and consequently promote cell proliferation and growth[39]. Moreover, we found that m6A modification are involved in regulating SOCS3 translation in a METTL3/ IGF2BP1-orchestrated manner. Consequently, we demonstrated that METTL3 promotes the m6A methylation of SOCS3 mRNA, and then IGF2BP1 recognizes and stabilizes SOCS3 mRNA and promotes SOCS3 protein expression. Consistently, a recent study have shown that the reduction of phosphorylation of JAK2/STAT3 in aged Klotho deficient (+/-) mice; however, the mechanism by which DR1 affecting the aging of cells has not been reported[40]. Our study that m6A methylation of SOCS3 regulate the senescence of SkMSCs through JAK2–STAT3 signaling. Epigenetic modification of m6A has a powerful influence on cellular senescence and affects the cell fate and leads to the overexpression of target protein in aged mice to relieve age-related disease; however, further exploration of the molecular mechanisms remain is required [41,42]. Our data provides the evidence that SOCS3 binds to JAK2 and promote its degradation.

Several limitations need be noted. Firstly, the role of SOCS3 to METTL3-mediated m6A methylation may vary due to cell type,cellular signal and microenvironment. Second, we have explored the association between m6A modification and SOCS3, however, we failed to identify the exact binding site of SOCS3 that interact with downstream target. Thirdly, Further in vivo study is needed to reveal the role of m6A and manipulation of m6A modification in senescence. Despite these limitations, our data have demonstrated that reduction of m6A is a senescence biomarker in SkMSCs and that the restoration of m6A through METTL3 upregulation can alleviate senescence of SkMSCs.

In summary, our study shows that IGF2BP1-mediated improvement of SOCS3 mRNA stability is enhanced by METTL3-mediated m6A methylation to alleviate the senescence of SkMSCs. The association between SOCS3 and m6A modification implies that the manipulation of m6A modification may serve as a promising treatment for age-related disease. Our present study provided the molecular mechanism of m^6A in aging and identifies METLL3 and SOCS3 as therapeutic target

for the diagnosis and treatment of age- associated disorders. Further studies are needed to identify the exact binding site of SOCS3 that interact with JAK2 and we speculate that SOCS3 may have other targets besides JAK2 in SkMSCs.

4 Materials And Methods

4.1 Cell culture *and transfection*

Female BALB/c mice were purchased from The Guangdong Medical Laboratory Animal Center as reported. Young and aged SkMSCs were obtained from 6-week-old and 6-month-old and were cultured in DMEM (Gibco; Thermo Fisher Scientific, Inc.) supplemented with 20% FBS (HyClone; GE Healthcare life Sciences)and 1% chick embryo extract (Gemini Bio Products). The overexpression vectors

(Qiagen/Exiqon) for METTL3 (METTL3-OE), SOCS3 (SOCS3-OE) and IGF2BP1 (IGF2BP1 -OE) and the Small interfering RNA (Bioss, Beijing, China) for METTL3 (METTL3-KO), SOCS3 (SOCS3-KO) and IGF2BP1(IGF2BP1-KO) were pretransfected into SkMSCs, respectively. The above vectors were delivered into SkMSCs by using a Lipofectamine 2000 reagent (Invitrogen, CA, USA) according to the manufacturer's instructions.

4.2 Clonal expansion assay

To assess the proliferative capacity of SkMSCs, clonal expansion assay was performed. Initially, cells were seeded in a six-well plate (Corning Inc) and cultured in the growth medium for 10 to 15 days, then fixed with 4% paraformaldehyde for 15 – 20 min. The cells were washed with phosphate buffer solution (PBS), treated with 0.2% crystal, and imaged using a microscope digital camera (Olympus).

4.3 Senescence-associated–galactosidase (SA-Gal) staining

SA-Gal staining was adopted to assess the senescence of SkMSCs. Briefly, the cultured cells were washed twice with PBS and fixed with 2% formaldehyde and 0.2% glutaraldehyde for 5 min at room temperature. The fixed cells were stained with SA-Gal staining solution (Cell Biolabs, USA) at 37°C without CO2 overnight and then calculated the percentage of SA-Gal positive cells.

4.4 Western blotting

Western blotting was performed as reported previously[43]. Briefly, proteins were extracted from cell lysates and were quantified with a BCA quantification kit (Thermo Fisher Scientific). Then, the samples were electrotransferred to PVDF membranes (Millipore) and were blocked and incubated with rabbit anti-GAPDH (1:1000; ab9485, Abcam, Cambridge, UK), anti-METTL3 (1:1000; ab195352), anti-METTL14 (1:1000; ab252562), anti-SOCS3 (1:1000; ab280884), anti-IGF2BP1(1:200, ab100999) antibodies overnight at 4°C. Following incubated with secondary antibody, the results were captured by ChemiDoc XRS system (Bio-Rad).

4.5 Immunofluorescence

Immunostaining was conducted according to the manufacturer's instructions. In brief, The samples were fixed with 4% paraformaldehyde, permeabilized with 0.4% Triton X-100, and blocked with 10% sheep serum. After the samples were incubated with the primary antibody and secondary antibody, respectively, they were subjected to Hoechst 33342 (Invitrogen). Images were captured with a microscope digital camera (Olympus).

4.6 RNA isolation and reverse transcription-quantitative polymerase chain reaction

(RT-qPCR) amplification

Total RNA extraction and amplification were performed as reported previously. Briefly, the samples were extracted using TRIzol reagent (Invitrogen), and then RNA was converted to cDNA with the SuperScript® cDNA Synthesis Kit (Thermo). The cDNA was then applied to the 7500HT Fast Real-Time PCR system (Applied Biosystems) and the 2× UltraSYBR Mixture (CW Bio) for q-PCR as follows: 15 min at 95°C and 40 cycles of 15 s at 95°C and 30 s at 60°C. The following primers were used: GAPDH forward 5'-ACTGAGGACCAGGTTGTC-3' and reverse 5'-TGCTGTAGCCGTATTCATTG-3'; METTL3 forward 5'-CAAGCTGCACTTCAGACGAA-3' and reverse 5'-GCTTGGCGTGTGGTCTTT-3', METTL14 forward 5 -TCTTCTTCATATGGCAAATTTTCTT-3 , and reverse 5 - TATCCCTCTTGGTCTGTGGAG-3 . Data were analyzed with SDS Software version 2.0 (Applied Biosystems).

4.7 MeRIP-seq

MeRIP was conducted by Guangzhou Bainuowei Biotechnology Co., LTD. Briefly, Purified mRNA was treated with DNase I (Sigma-Aldrich) and fragmented into ≤ 100 bp fragments using an RNA fragmentation reagent (Thermo Fisher, Carlsbad, CA, USA). Approximately one-tenth of the RNA was used as the input control for further RNA sequencing using RiboBio (Guangzhou, China). Anti-m6A antibody was mixed with Protein A Dynabeads (Invitrogen) followed by addition of the mRNA fragments. The mixture was mixed with prewashed Pierce™ Protein A/G Magnetic Beads (Invitrogen) in immunoprecipitation buffer (Sigma-Aldrich), followed by RNA extraction using phenol:chloroform (Thermo Fisher, Carlsbad, CA, USA). The methylated RNA was purified for MeRIP-seq using RiboBio (Guangzhou, China).

The MeRIP-seq data were analyzed according to the published standardized pipeline. MACS (version 1.4) was used for peak detection. m6A peaks were measured by the ExomePeak software (v2.6.0). RNA-seq reads were normalized using Cufflinks (v2.2.1), and Cuffdiff was used to determine the differentially expressed genes.

4.8 RIP-qPCR

RIP was performed using Magna MeRIP m6A Kit (Millipore, Germany) according to the manufacturer's instructions. In brief, RNA was isolated from young and aged SkMSCs using Dynabeads™ mRNA Purification Kit (Invitrogen), and one-tenth of the RNA was used as the control. The RNA was incubated with m6A-specific antibody (Abcam) in immunoprecipitation buffer with RNase inhibitors; the complexes were incubated with Pierce ™ Protein A/G Magnetic Beads (Thermo Scientific) for 2 h at 4°C with rotation. Based on the MeRIP-seq results, enrichment was evaluated using qPCR. The corresponding m6A enrichment in each sample was calculated by normalizing it to that in the input control. Genes differentially expressed between young and aged SkMSCs or between control and METTL3-knockout SkMSCs were determined using the R-package DEseq2 software. The relative enrichment of m6A was normalized to that in the input control as follows: % input = 1/10 × 2Ct [IP] – Ct [input].

4.9 RNA stability analysis

RNA stability analysis was performed according to the manufacturer's instructions. SkMSCs were cultured in six-well plates. Actinomycin D (Apexbio, USA) was added at a final concentration of 5 g/ml. Total RNA was extracted with TRIzol reagent (Thermo Fisher Scientific, USA). RT-qPCR was performed as previously reported and each RNA transcript of interest and its RNA half-life (t(1/2)) were determined using ln2/slope and GAPDH was used for normalization.

4.10 Liquid chromatography-tandem mass spectrometry (LC-MS/MS)

Quantification was performed using LC–MS/MS on an Agilent system according to the manufacturer's instructions. Briefly, 100 ng of mRNA was treated with a mixture of nuclease P1 and calf intestinal phosphatase (1:10) overnight at 37°C. The mixture was neutralized using HCl; samples were filtered through a 0.22 μm filter (Millipore) and subjected to LC–MS/MS analysis. The samples were then separated through LC on a C18 column (Agilent) using a Biosystems 6500 Triple Quadrupole (Agilent Technologies). Quantification was performed using standard curves obtained from standards run with the same batches of samples. RNA modification levels were determined by MetWare according to the LC-MS/MS platform.

4.11 Statistical analysis

Statistical significance was determined by Student's t-test for comparisons between two groups and by one-way analysis of variance followed by Tukey's post hoc test for comparisons between more than two groups using the Prism software package version 8.4 (GraphPad Software, La Jolla, CA). $P < 0.05$ was determined to indicate a statistically significant difference.

Declarations

Acknowledgement

We thank Professor Weiyi Fang for assistance about MeRIP-seq experiment.We thank Professor Longyuan Li for the suggestions about bioinformatic analysis. This study was supported by Youth Start-Up Fund(grant nos. QN2020005) and The Natural Science Foundation of Guangdong Province (grant nos. 2018A030310254 and 2015A030310350).

Authors' contributions

MZ and YY carried out experiments, data analysis and wrote the manuscript. BQ and GC performed experiments and helped with data quantifications. LG and JY designed the project and supervised the experiment. All authors read and approved the final manuscript.

Competing interests

The authors declare that they have no competing interests.

Availability of data and materials

The datasets used and/or analyzed during the current study are included either in this article or in the supplementary information files.

Ethics approval and consent to participate

The study was approved by the Ethics Review Committee of The Third Affiliated Hospital of Southern Medical University (Guangzhou, China). The animal study followed the Guidelines for the Animal Care and Use approved by The Third Affiliated Hospital of Southern Medical University.

References

1. Poh, H. X., Mirza, A. H., Pickering, B. F. & Jaffrey, S. R. Alternative splicing of METTL3 explains apparently METTL3-independent m6A modifications in mRNA. *PLoS biology* **20**, e3001683, doi:10.1371/journal.pbio.3001683 (2022).
2. Li, G. *et al.* m6A hypomethylation of DNMT3B regulated by ALKBH5 promotes intervertebral disc degeneration via E4F1 deficiency. *Clinical and translational medicine* **12**, e765, doi:10.1002/ctm2.765 (2022).
3. Yoneda, R., Ueda, N. & Kurokawa, R. m(6)A Modified Short RNA Fragments Inhibit Cytoplasmic TLS/FUS Aggregation Induced by Hyperosmotic Stress. *International journal of molecular sciences* **22**, doi:10.3390/ijms222011014 (2021).
4. Ghosh, G. *et al.* Poly C Binding Protein 2 dependent nuclear retention of the utrophin-A mRNA in C2C12 cells. *RNA biology* **18**, 612-622, doi:10.1080/15476286.2021.2004683 (2021).
5. Wu, Z. *et al.* METTL3 counteracts premature aging via m6A-dependent stabilization of MIS12 mRNA. *Nucleic acids research* **48**, 11083-11096, doi:10.1093/nar/gkaa816 (2020).
6. Yang, W. *et al.* Msi2-mediated MiR7a-1 processing repression promotes myogenesis. *Journal of cachexia, sarcopenia and muscle* **13**, 728-742, doi:10.1002/jcsm.12882 (2022).
7. Cho, S. *et al.* mTORC1 promotes cell growth via m(6)A-dependent mRNA degradation. *Molecular cell* **81**, 2064-2075 e2068, doi:10.1016/j.molcel.2021.03.010 (2021).
8. Mapperley, C. *et al.* The mRNA m6A reader YTHDF2 suppresses proinflammatory pathways and sustains hematopoietic stem cell function. *The Journal of experimental medicine* **218**, doi:10.1084/jem.20200829 (2021).
9. Chen, X. *et al.* METTL3-mediated m(6)A modification of ATG7 regulates autophagy-GATA4 axis to promote cellular senescence and osteoarthritis progression. *Annals of the rheumatic diseases* **81**, 87-99, doi:10.1136/annrheumdis-2021-221091 (2022).
10. Min, K. W. *et al.* Profiling of m6A RNA modifications identified an age-associated regulation of AGO2 mRNA stability. *Aging Cell* **17**, e12753, doi:10.1111/acel.12753 (2018).

11. Petrosino, J. M. *et al.* The m(6)A methyltransferase METTL3 regulates muscle maintenance and growth in mice. *Nat Commun* **13**, 168, doi:10.1038/s41467-021-27848-7 (2022).
12. Gheller, B. J. *et al.* A defined N6-methyladenosine (m(6)A) profile conferred by METTL3 regulates muscle stem cell/myoblast state transitions. *Cell death discovery* **6**, 95, doi:10.1038/s41420-020-00328-5 (2020).
13. Farup, J. *et al.* Human skeletal muscle CD90(+) fibro-adipogenic progenitors are associated with muscle degeneration in type 2 diabetic patients. *Cell metabolism* **33**, 2201-2214 e2211, doi:10.1016/j.cmet.2021.10.001 (2021).
14. Leung, C. *et al.* Lgr5 Marks Adult Progenitor Cells Contributing to Skeletal Muscle Regeneration and Sarcoma Formation. *Cell reports* **33**, 108535, doi:10.1016/j.celrep.2020.108535 (2020).
15. Kiss, T. *et al.* Nicotinamide mononucleotide (NMN) supplementation promotes anti-aging miRNA expression profile in the aorta of aged mice, predicting epigenetic rejuvenation and anti-atherogenic effects. *GeroScience* **41**, 419-439, doi:10.1007/s11357-019-00095-x (2019).
16. Roy, R. *et al.* DNA methylation signatures reveal that distinct combinations of transcription factors specify human immune cell epigenetic identity. *Immunity* **54**, 2465-2480 e2465, doi:10.1016/j.immuni.2021.10.001 (2021).
17. Gonzales, M. M. *et al.* Biological aging processes underlying cognitive decline and neurodegenerative disease. *The Journal of clinical investigation* **132**, doi:10.1172/JCI158453 (2022).
18. Grenov, A. C. *et al.* The germinal center reaction depends on RNA methylation and divergent functions of specific methyl readers. *The Journal of experimental medicine* **218**, doi:10.1084/jem.20210360 (2021).
19. Uddin, M. B., Wang, Z. & Yang, C. The m(6)A RNA methylation regulates oncogenic signaling pathways driving cell malignant transformation and carcinogenesis. *Molecular cancer* **20**, 61, doi:10.1186/s12943-021-01356-0 (2021).
20. Tassinari, V. *et al.* ADAR1 is a new target of METTL3 and plays a pro-oncogenic role in glioblastoma by an editing-independent mechanism. *Genome biology* **22**, 51, doi:10.1186/s13059-021-02271-9 (2021).
21. Alain, C. *et al.* Aging Enhances Neural Activity in Auditory, Visual, and Somatosensory Cortices: The Common Cause Revisited. *The Journal of neuroscience : the official journal of the Society for Neuroscience* **42**, 264-275, doi:10.1523/JNEUROSCI.0864-21.2021 (2022).
22. Shafik, A. M. *et al.* N6-methyladenosine dynamics in neurodevelopment and aging, and its potential role in Alzheimer's disease. *Genome biology* **22**, 17, doi:10.1186/s13059-020-02249-z (2021).
23. Kan, L. *et al.* A neural m(6)A/Ythdf pathway is required for learning and memory in Drosophila. *Nat Commun* **12**, 1458, doi:10.1038/s41467-021-21537-1 (2021).
24. Nazio, F. *et al.* Targeting cancer stem cells in medulloblastoma by inhibiting AMBRA1 dual function in autophagy and STAT3 signalling. *Acta neuropathologica* **142**, 537-564, doi:10.1007/s00401-021-02347-7 (2021).

25. Liu, Z. K. *et al.* EYA2 suppresses the progression of hepatocellular carcinoma via SOCS3-mediated blockade of JAK/STAT signaling. *Molecular cancer* **20**, 79, doi:10.1186/s12943-021-01377-9 (2021).
26. Pastoret, C. *et al.* Linking the KIR phenotype with STAT3 and TET2 mutations to identify chronic lymphoproliferative disorders of NK cells. *Blood* **137**, 3237-3250, doi:10.1182/blood.2020006721 (2021).
27. Benito-Villalvilla, C. *et al.* Allergoid-mannan conjugates reprogram monocytes into tolerogenic dendritic cells via epigenetic and metabolic rewiring. *The Journal of allergy and clinical immunology* **149**, 212-222 e219, doi:10.1016/j.jaci.2021.06.012 (2022).
28. Pelham, S. J. *et al.* STAT5B restrains human B-cell differentiation to maintain humoral immune homeostasis. *The Journal of allergy and clinical immunology*, doi:10.1016/j.jaci.2022.04.011 (2022).
29. Li, H. B. *et al.* m(6)A mRNA methylation controls T cell homeostasis by targeting the IL-7/STAT5/SOCS pathways. *Nature* **548**, 338-342, doi:10.1038/nature23450 (2017).
30. Li, Z. *et al.* YTHDF1 Negatively Regulates Treponema pallidum-Induced Inflammation in THP-1 Macrophages by Promoting SOCS3 Translation in an m6A-Dependent Manner. *Frontiers in immunology* **13**, 857727, doi:10.3389/fimmu.2022.857727 (2022).
31. Castellanos-Rubio, A. *et al.* A novel RT-QPCR-based assay for the relative quantification of residue specific m6A RNA methylation. *Scientific reports* **9**, 4220, doi:10.1038/s41598-019-40018-6 (2019).
32. Kanellis, D. C. *et al.* The exon-junction complex helicase eIF4A3 controls cell fate via coordinated regulation of ribosome biogenesis and translational output. *Science advances* **7**, doi:10.1126/sciadv.abf7561 (2021).
33. Wang, S. *et al.* The Combined Effects of Circular RNA Methylation Promote Pulmonary Fibrosis. *American journal of respiratory cell and molecular biology* **66**, 510-523, doi:10.1165/rcmb.2021-0379OC (2022).
34. Wei, W. *et al.* Circ0008399 Interaction with WTAP Promotes Assembly and Activity of the m(6)A Methyltransferase Complex and Promotes Cisplatin Resistance in Bladder Cancer. *Cancer research* **81**, 6142-6156, doi:10.1158/0008-5472.CAN-21-1518 (2021).
35. Zhou, X. *et al.* EIF4A3-induced circFIP1L1 represses miR-1253 and promotes radiosensitivity of nasopharyngeal carcinoma. *Cellular and molecular life sciences : CMLS* **79**, 357, doi:10.1007/s00018-022-04350-x (2022).
36. Otani, Y., Fujita, K. I., Kameyama, T. & Mayeda, A. The Exon Junction Complex Core Represses Cancer-Specific Mature mRNA Re-splicing: A Potential Key Role in Terminating Splicing. *International journal of molecular sciences* **22**, doi:10.3390/ijms22126519 (2021).
37. Fatima, I. *et al.* Skin Aging in Long-Lived Naked Mole-Rats is Accompanied by Increased Expression of Longevity-Associated and Tumor Suppressor Genes. *The Journal of investigative dermatology*, doi:10.1016/j.jid.2022.04.028 (2022).
38. Du, X. *et al.* Deletion of Socs3 in LysM(+) cells and Cx3cr1 resulted in age-dependent development of retinal microgliopathy. *Molecular neurodegeneration* **16**, 9, doi:10.1186/s13024-021-00432-9 (2021).

39. Yang, Z., Cai, Z., Yang, C., Luo, Z. & Bao, X. ALKBH5 regulates STAT3 activity to affect the proliferation and tumorigenicity of osteosarcoma via an m6A-YTHDF2-dependent manner. *EBioMedicine* **80**, 104019, doi:10.1016/j.ebiom.2022.104019 (2022).
40. Nguyen, B. T. *et al.* Ginsenoside Re attenuates memory impairments in aged Klotho deficient mice via interactive modulations of angiotensin II AT1 receptor, Nrf2 and GPx-1 gene. *Free radical biology & medicine* **189**, 2-19, doi:10.1016/j.freeradbiomed.2022.07.003 (2022).
41. Cai, G. P. *et al.* Alkbh1-mediated DNA N6-methyladenine modification regulates bone marrow mesenchymal stem cell fate during skeletal aging. *Cell proliferation* **55**, e13178, doi:10.1111/cpr.13178 (2022).
42. Li, X. *et al.* Cap-independent translation of GPLD1 enhances markers of brain health in long-lived mutant and drug-treated mice. *Aging Cell*, e13685, doi:10.1111/acel.13685 (2022).
43. Zhu, M., Lian, C., Chen, G., Zou, P. & Qin, B. G. CircRNA FUT10 regulates the regenerative potential of aged skeletal muscle stem cells by targeting HOXA9. *Aging* **13**, 17428-17441, doi:10.18632/aging.203233 (2021).

Figures

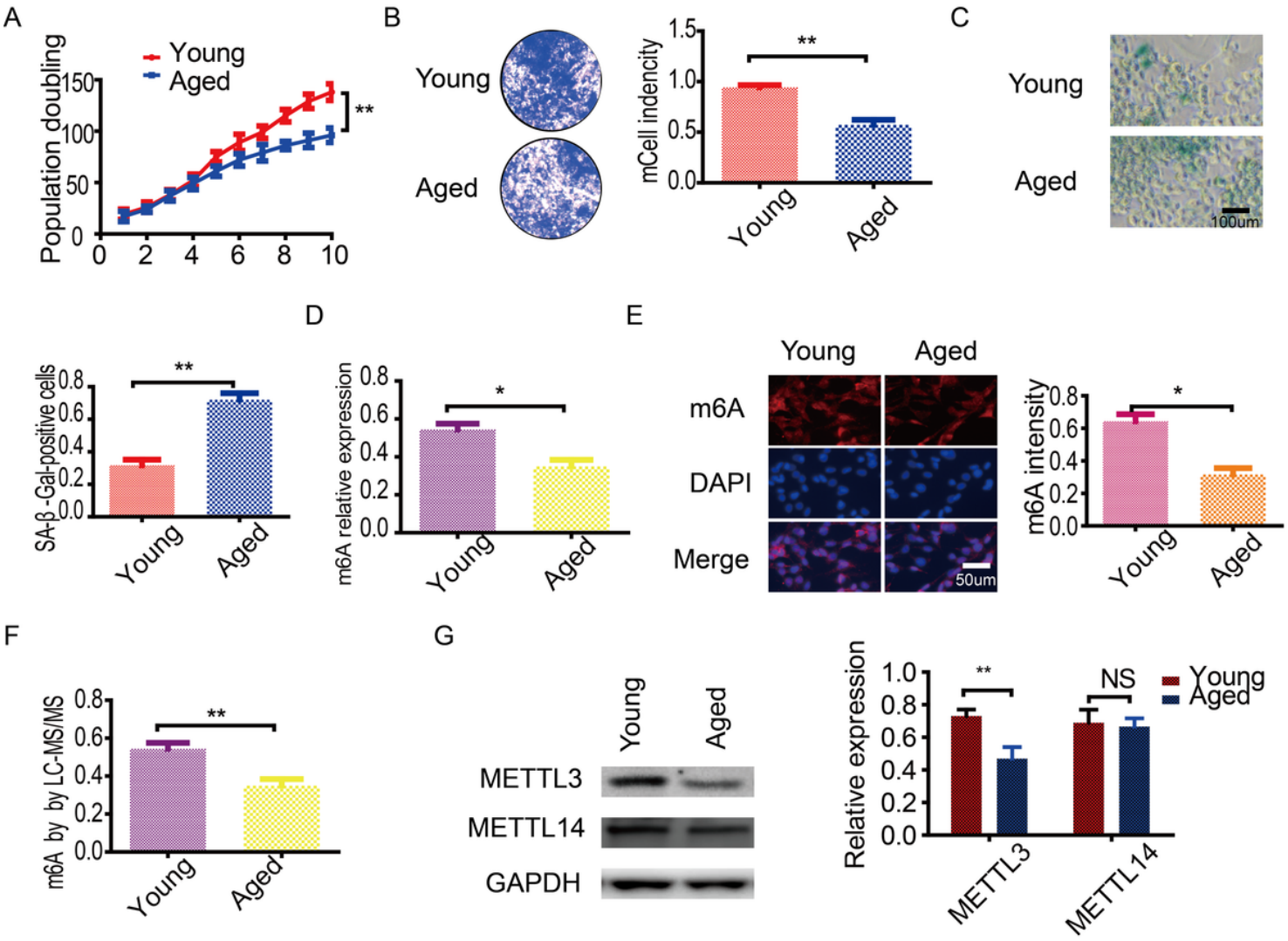

Figure 1

Decreased m6A methylation in aged SkMSCs. (A) MTT analysis to assesse the proliferative potential of adult and aged SkMSCs. (B) Clonal formation assay in adult aged SkMSCs. (C) SA-Gal staining of adult and aged SkMSCs. (D) Western blot showing m6A levels in SkMSCs. (E) Immunostaining for m6A expression in SkMSCs. (F) LC–MS/MS measured the level of m6A in SkMSCs. (G) Western blot analysis of METTL3 and METTL14 expression in young and aged SkMSCs. Data are presented as mean ±SEM; n = 3. *P < 0.05; **P < 0.01; NS, not significant. All experiments were performed at least three times with duplication within each individual experiment.

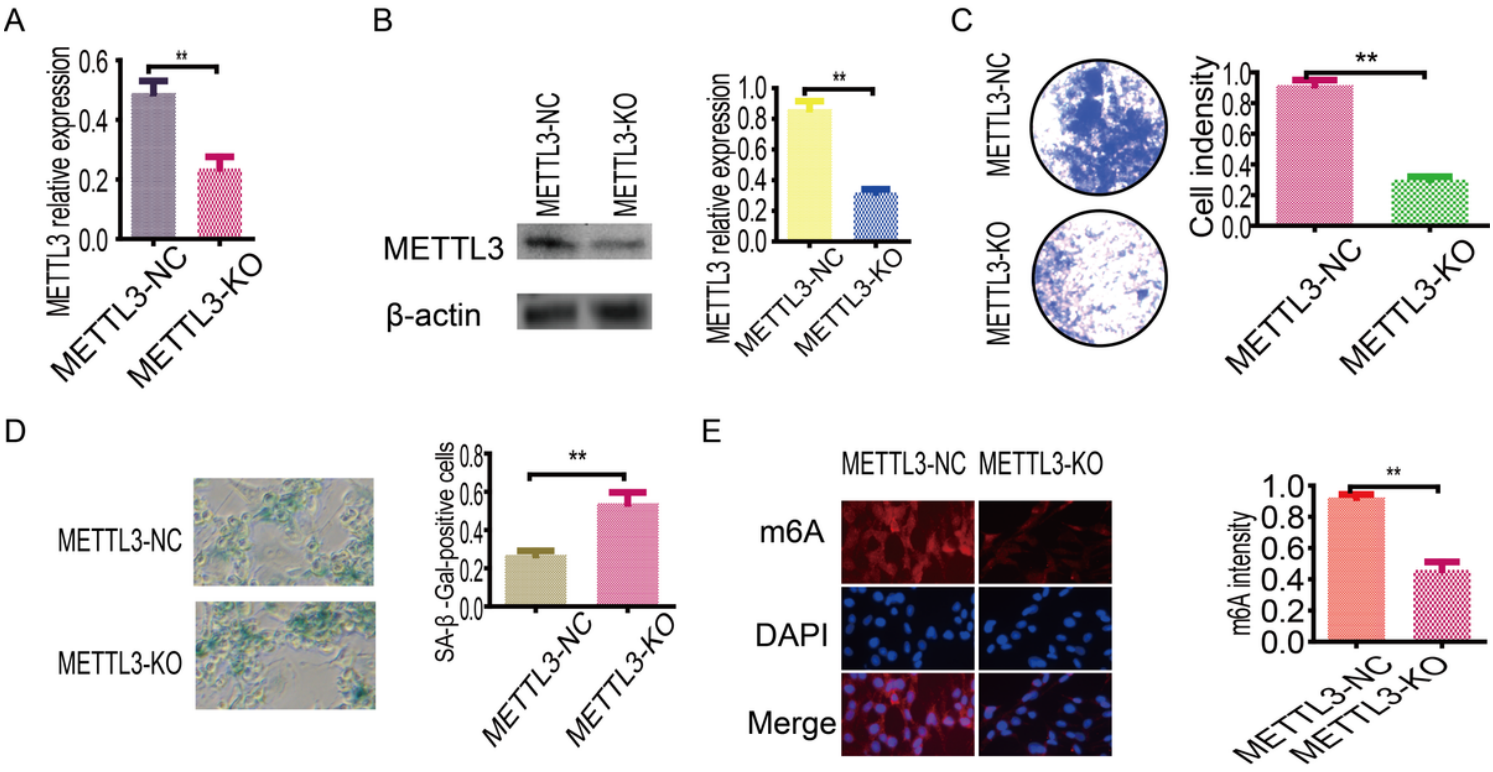

Figure 2

Reduction of METTL3 promote senescence in SkMSCs. (A) METTL3 expression in METTL3-NC and METTL3-KO group. (B) Western blot showing METTL3 in METTL3-NC and METTL3-KO group. (C) Clonal formation showing the proliferation of SkMSCs in METTL3-NC and METTL3-KO groups. (D) SA-β-Gal staining for SkMSCs in METTL3-NC and METTL3-KO group. (E) Immunostaining for m6A modification in METTL3-NC and METTL3-KO group in SkMSCs.

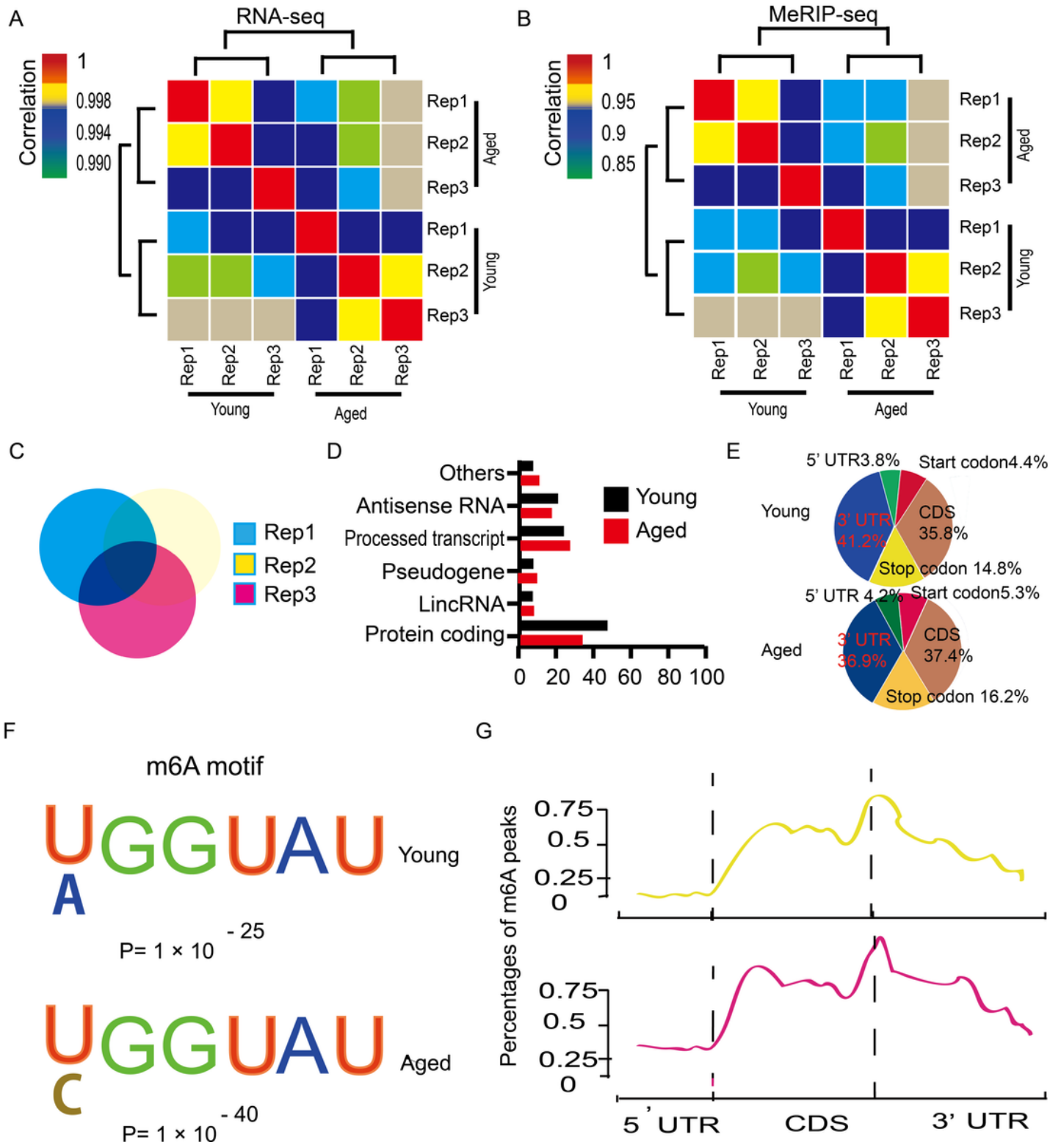

Figure 3

Characterization of m6A mRNA methylation in young and aged SkMSCs. (A) Heatmap depicting the Pearson's correlation coefficients of RNA-seq data acorss young and aged SkMSCs samples. The samples were hierarchically clustered. (B) Heatmap depicting the Pearson's correlation coefficients of MeRIP-seq data acorss young and aged SkMSCs samples. The samples were hierarchically clustered. (C) Venn diagram showing the overlap in numbers and percentages of m6A peaks detected from two

independent replicates in young and aged SkMSCs. (D) Distribution of m6A-tagged transcript types as identified by MeRIP-seq in young and aged SkMSCs. (E) Pie chart showing the fraction of m6A peaks in different transcript segments. (F) m6A motif identified in adult and aged SkMSCs. (G) Distribution of m6A peaks in the 5'untranslated region (UTRs), coding sequences (CDSs), and 3' UTRs of total mRNA from young and aged SkMSCs.

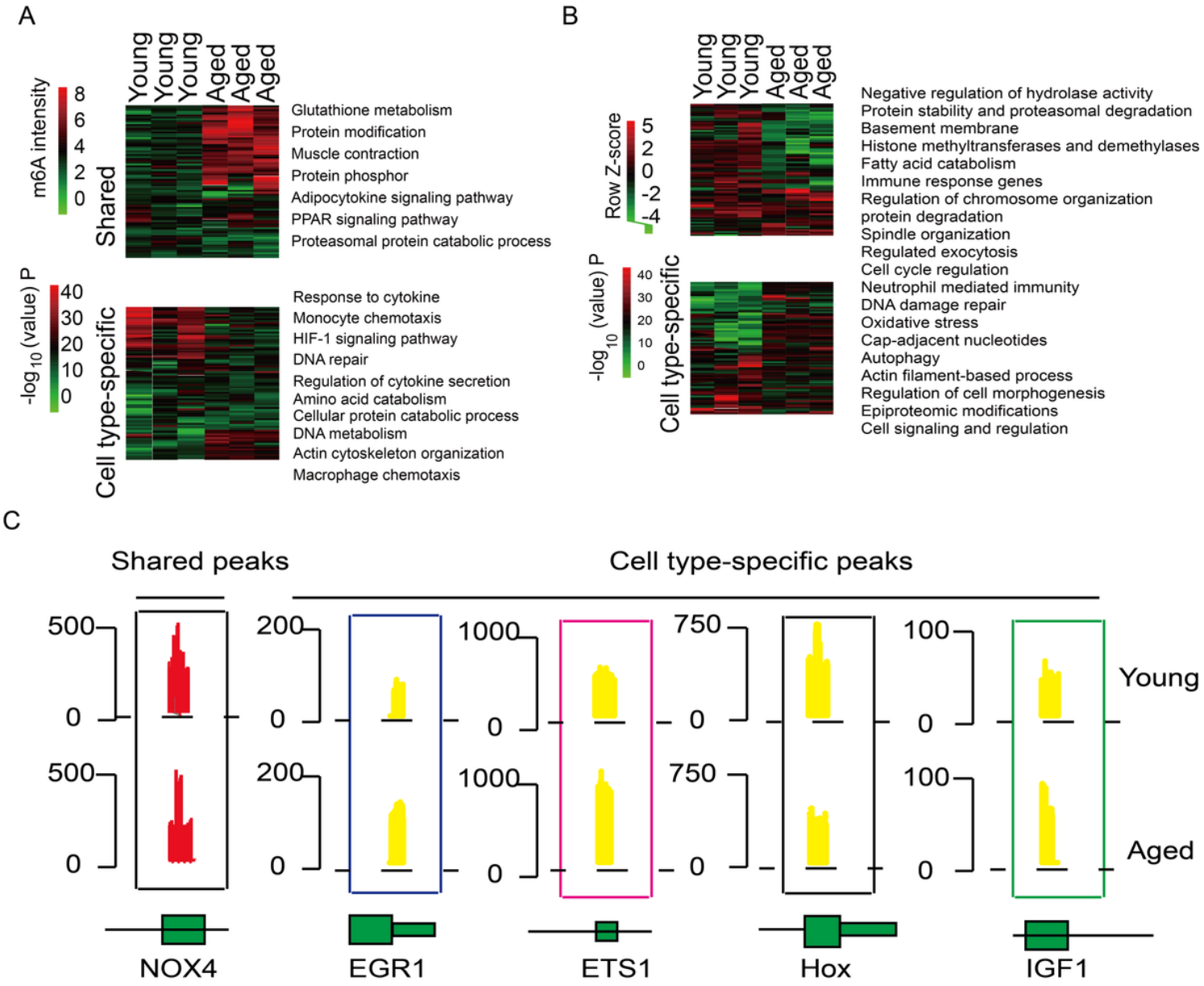

Figure 4

m6A profiling in adult and aged SkMSCs. (A) Shared and specific m6A peaks in young and aged SkMSCs. (B) Clustering of differentially expressed genes in young and aged SkMSCs. (C) Representative examples of shared and specific m6A peaks.

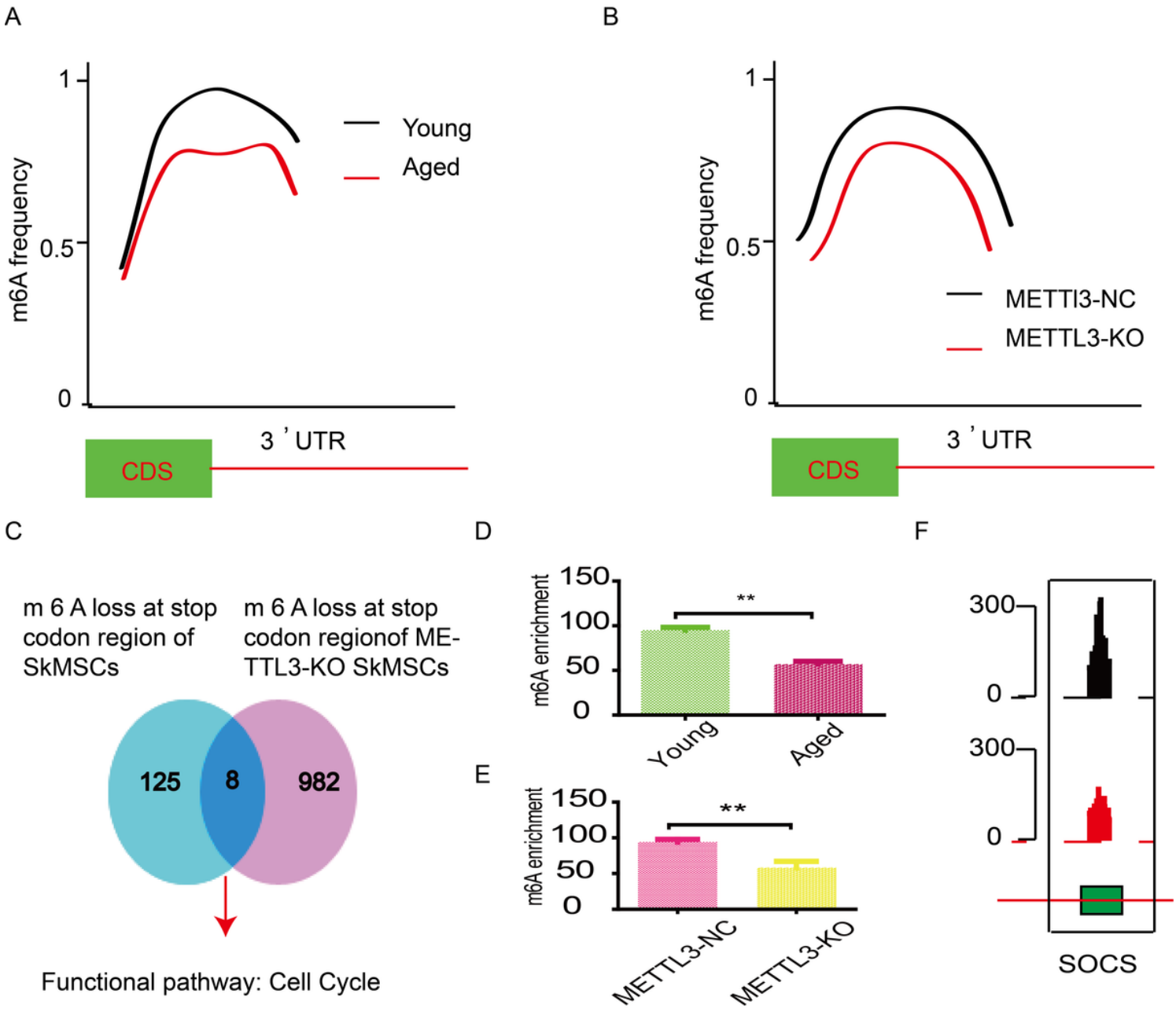

Figure 5

SOCS3 is a target of METTL3 regulating SkMSCs senescence. (A) The frequency of m6A flanking the stop codons in transcripts from young and aged SkMSCs. (B) m6A frequency in regions flanking the stop codon regions in the METTL3-KO and control groups. (C) Pie chart showing genes that overlap between the METTL3-KO and METTL3-NC groups. (D) m6A modification on SOCS3 mRNA in young and aged SkMSCs. (E) MeRIP-qPCR showing m6A enrichment in SOCS33 mRNA of METTL3-KO and METTL3-NC groups. (F) MeRIP-qPCR showing m6A enrichment on SOCS3 mRNA of the METTL3-KO and METTL3-NC groups.

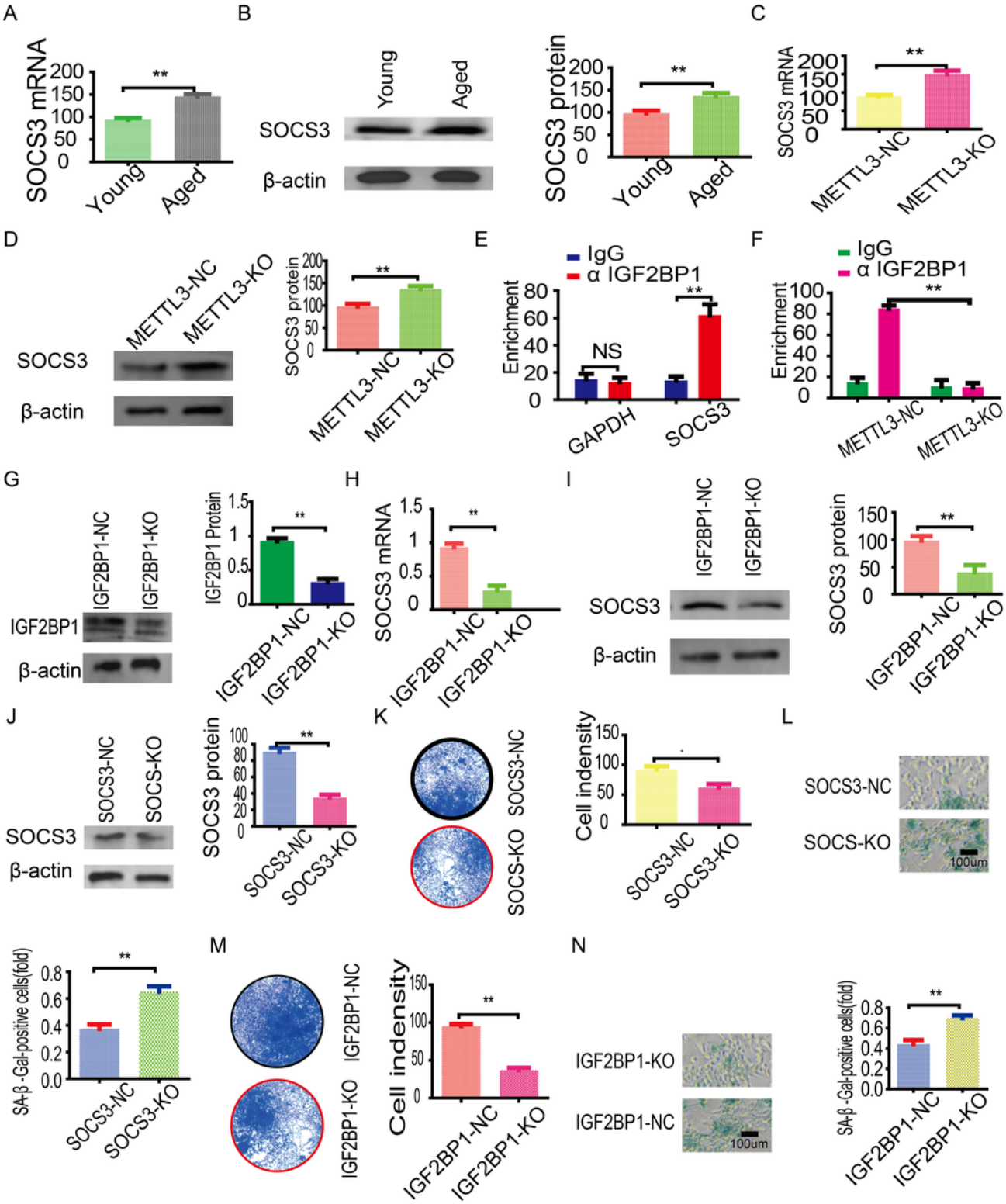

Figure 6

m6A accelerated IGF2BP1-mediated SOCS3 mRNA stability and relieved senescence in SkMSCs. (A) q-PCR showing SOCS3 mRNA levels in young and aged SkMSCs. (B) Western blotting showing SOCS3 protein levels in young and aged SkMSCs. (C) qPCR showing SOCS3 mRNA levels in METTL3-NC and METTL3-KO SkMSCs. (D) Western bloting showing SOCS3 protein expression in METTL3-NC and METTL3-KO groups. (E) RIP-qPCR showing IGF2BP1 enrichment in SOCS3 mRNA in SkMSCs. (F) RIP-

qPCR analysis showing enrichment of IGF2BP1 in SOCS3 mRNA in METTL3-NC and METTL3-KO SkMSCs. (G) Western blot showing IGF2BP1 levels in IGF2BP1-NC and IGF2BP1-KO groups. (H) qPCR showing SOCS3 levels in IGF2BP1-NC and IGF2BP1-KO groups. (I) Western blot showing SOCS3 levels in control and IGF2BP1-KO groups. (J) Western blot showing SOCS3 levels in SOCS3-NC and SOCS3-knockout (SOCS3-KO) groups. (K) Clonal formation assay in control and SOCS3-KO groups. (L) SA-β-Gal staining showing cell senescence in SOCS3-NC and SOCS3-KO groups. (M) Clonal formation assay showing cell proliferation in IGF2BP1-NC and IGF2BP1-KO groups. (N) SA-β-Gal staining showing cell senescence in IGF2BP1-NC and IGF2BP1-KO groups.

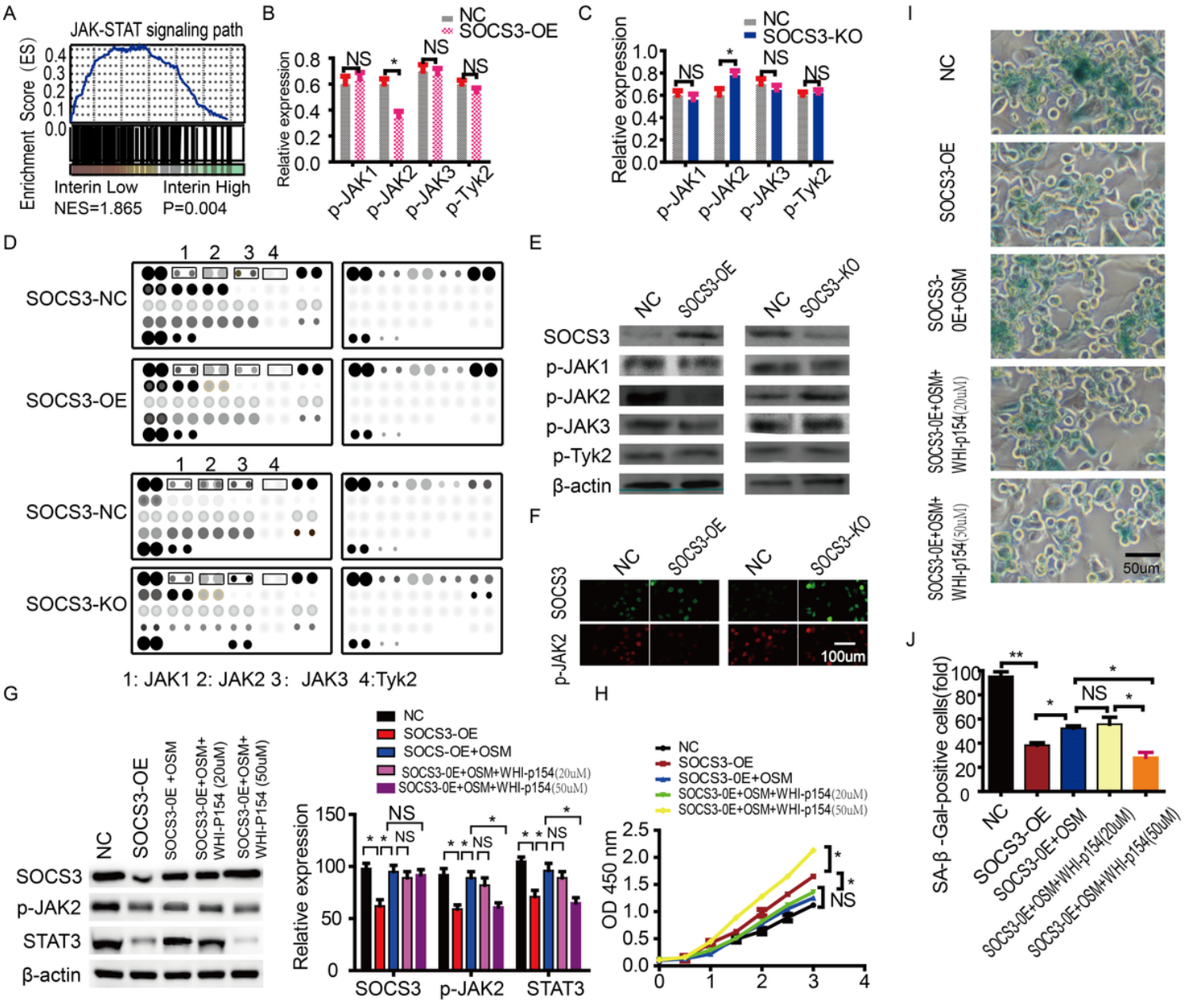

Figure 7

Identification of extracellular JAK as a regulatory target of SOCS3. (A) GSEA identified a significant correlation between SOCS3 and the JAK signaling pathway. (B–D) Phospho-kinase microarray assay

showing conditioned medium from stably transfected SkMSCs. (E) Crucial members of the JAK–STAT signaling pathway were examined by western blotting. (F) Representative images of SOCS3 and phosphorylated JAK immunostaining in SkMSCs. (G) Downstream effectors of JAK2 signaling were examined by western blotting. (H) Effect of SOCS3 downregulation on SkMSC proliferation. (I-J) SA-β-Gal staining of SkMSCs.

Supplementary Files

This is a list of supplementary files associated with this preprint. Click to download.

- Supplement.doc
- FigureS1.tif
- FigureS2.tif
- FigureS3.tif
- FigureS4.tif
- FigureS5.tif